

Cite this: DOI: 10.1039/c2dt30852e

www.rsc.org/dalton

PAPER

## An 1,3,4-oxadiazole-based OFF–ON fluorescent chemosensor for Zn<sup>2+</sup> in aqueous solution and imaging application in living cells†

Ji-An Zhou,<sup>a</sup> Xiao-Liang Tang,<sup>a</sup> Ju Cheng,<sup>b</sup> Zheng-Hua Ju,<sup>a</sup> Li-Zi Yang,<sup>a</sup> Wei-Sheng Liu,<sup>\*a</sup> Chun-Yang Chen<sup>a</sup> and De-Cheng Bai<sup>b</sup>

Received 18th April 2012, Accepted 27th June 2012

DOI: 10.1039/c2dt30852e

A new 1,3,4-oxadiazole-based fluorescence chemosensor **1**, *N*-(2-ethoxy-2-oxoethyl)-*N*-(5-(2-hydroxy-3,5-di-*tert*-butylphenyl)-[1,3,4]oxadiazol-2-yl)glycine ethyl ester, has been designed and synthesized. Its fluorescence properties and selectivity for various metal ions were investigated in detail. A prominent fluorescence enhancement only for Zn<sup>2+</sup> was found in aqueous acetonitrile solution and the response mechanism of **1** was analyzed by time-resolved fluorescence decay and DFT calculations. Furthermore, the fluorescence imaging of Zn<sup>2+</sup> in living cells was successfully applied.

### Introduction

Selective detection or quantification of metal ions is an area of growing interest in supramolecular chemistry due to its importance in a wide range of environmental, clinical, chemical, and biological applications.<sup>1</sup> As the second-most abundant transition metal ion in the human body for sustaining life, Zn<sup>2+</sup> is actively involved in various biological processes in several organs, *e.g.*, brain, pancreas, spermatozoa, vesicles of presynaptic neurons, *etc.*, and plays pivotal roles in controlling gene transcription and metalloenzyme function in either a free state or a sequestered form.<sup>2</sup> Disruption of Zn<sup>2+</sup> homeostasis may be implicated in a number of severe neurological diseases such as Alzheimer's disease, amyotrophic lateral sclerosis, Guam ALS-Parkinsonism-dementia Parkinson's disease, hypoxia ischemia, and epilepsy.<sup>2,3</sup> Up to now, fluorescence detection has been regarded as the most effective means to monitor Zn<sup>2+</sup> in biological systems because of its special 3d<sup>10</sup>4s<sup>0</sup> electronic configuration, which does not give any spectroscopic or magnetic signals.<sup>4</sup>

In the last decades, considerable efforts have been made towards the design and synthesis of various fluorescent chemosensors for the *in vitro* and *in vivo* detection of Zn<sup>2+</sup>.<sup>5</sup> The common probes are derivatives of quinoline,<sup>6</sup> fluorescein,<sup>7</sup> coumarin,<sup>8</sup> anthracene,<sup>9</sup> dipicolylamine,<sup>10</sup> macrocycle,<sup>11</sup> Schiff-base family,<sup>12</sup> and so on.<sup>5</sup> However, some of them have characteristic

poor water solubility, which inevitably hinders their applications. Many of the available sensors have difficulty in distinguishing Zn<sup>2+</sup> from Ca<sup>2+</sup>, Mg<sup>2+</sup> or Cd<sup>2+</sup>, which compete with Zn<sup>2+</sup> for the binding sites of the sensor molecule. Especially, Cd<sup>2+</sup> is in the same group of the periodic table and has similar properties with Zn<sup>2+</sup>, which results in similar fluorescence changes when Zn<sup>2+</sup> and Cd<sup>2+</sup> are coordinated with fluorescent sensors.<sup>13</sup> In addition, it is necessary to control the chemosensors exhibiting fluorescence enhancement (OFF–ON) rather than fluorescence quenching (ON–OFF) for sensitivity reasons, which could eliminate the attenuation of testing signals arising from some interfering constituents in the environment as much as possible.<sup>14</sup> Therefore, there is a huge scope and potential for exploring novel OFF–ON fluorescent chemosensors for highly selective and sensitive determination of Zn<sup>2+</sup> in biological samples to understand the physiological functions of Zn<sup>2+</sup>.

Aromatic 1,3,4-oxadiazoles consisting of five-membered heterocyclic not only exhibit relevant biological properties and a wide variety of applications in the field of medicine and agriculture,<sup>15</sup> but also have been used as laser dyes, photographic materials or scintillators during past decades.<sup>16</sup> In recent years, their use has grown rapidly in the application of some 1,3,4-oxadiazoles in coordination chemistry and structural studies of supramolecule polymers.<sup>17</sup> However, to the best of our knowledge, the coordination properties of 1,3,4-oxadiazoles with metal ions have been rarely introduced into fluorescent chemosensor research so far.

In this paper, we present an aromatic 1,3,4-oxadiazole-based chelation-enhanced fluorescence (CHEF) system **1** as a highly selective fluorescent sensor for Zn<sup>2+</sup> in aqueous solution. The chemosensor was designed to involve three parts: a 3,5-di-*tert*-butylphenyl electron-rich unit, 2-hydroxy-phenyl-1,3,4-oxadiazole chelator (binding unit and potential fluorophore), and membrane-permeable auxiliary. It is expected that suitable metal ion could effectively act as an electrophile and attack the hydroxyl oxygen atom with electron-rich property and torsional motions

<sup>a</sup>Key Laboratory of Nonferrous Metal Chemistry and Resources Utilization of Gansu Province and State Key Laboratory of Applied Organic Chemistry, College of Chemistry and Chemical Engineering, Lanzhou University, Lanzhou, 730000, P. R. China.  
E-mail: liuws@lzu.edu.cn; Fax: +86-931-8912582;  
Tel: +86-931-8915151

<sup>b</sup>School of Basic Medical Sciences, Lanzhou University, Lanzhou, 730000, P. R. China

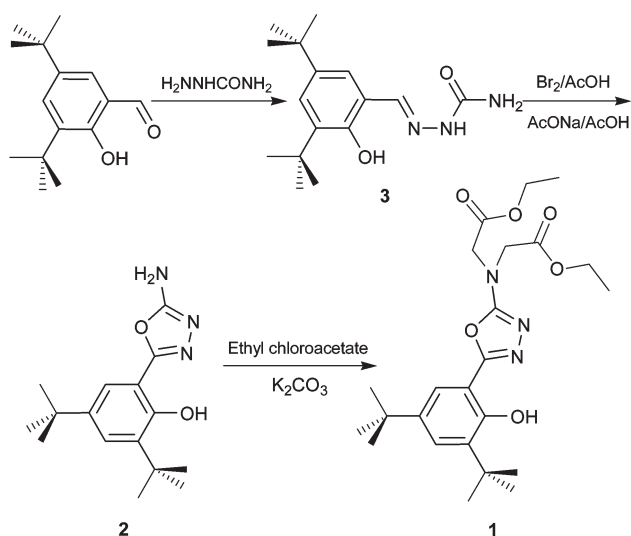
† Electronic supplementary information (ESI) available: The experimental methods, equations, characterisation data, supplementary spectra, NMR, MS spectra, DFT calculation data, radiative and the total non-radiative rate data. See DOI: 10.1039/c2dt30852e

of the two aryl moieties in 2-hydroxy-phenyl-1,3,4-oxadiazole group could be prevented, accompanied by the formation of a rigid planar metal complex structure and simultaneous metal-induced block of non-radiative transitions to turn on the fluorescence signal. Therefore, the fluorescence properties and highly selectivity of **1** for  $\text{Zn}^{2+}$  over other possible competitive cations were investigated in detail, and *in vivo* fluorescence imaging of  $\text{Zn}^{2+}$  in living cells was also successfully applied and tested.

## Results and discussion

The synthesis of **1** is shown in Scheme 1 (see the ESI†). Reaction of 3,5-di-*tert*-butyl-2-hydroxybenzaldehyde with semicarbazide in refluxing ethanol affords 1-(3,5-di-*tert*-butyl-2-hydroxybenzylidene)semicarbazide **3** with 89.3% yield, then compound **2** was prepared by using  $\text{Br}_2$  in acetic acid. **1** as a pale yellow viscous liquid was synthesized *via* a simple one-step reaction of **2** with 5 equiv of ethyl chloroacetate in good yield in the presence of anhydrous potassium carbonate in refluxing acetonitrile (75.0%). The purity of **1** was fully confirmed by  $^1\text{H}$ ,  $^{13}\text{C}$  NMR and ESI-MS analysis.

Sensor **1** exhibits a single emission band at 425 nm and weaker fluorescence with quantum yield ( $\Phi$ ) *ca.* 0.123 in the aprotic acetonitrile solvent, which is different from the fluorescence properties of those similar molecules, such as 2-(2'-hydroxyphenyl)benzoxazole (HPBO) derivatives with dual wavelength emission due to excited-state proton transfer (ESIPT) processes.<sup>13b,18</sup> For **1**, the presence of 3,5-di-*tert*-butylphenyl leads to electron-rich properties and weak acidity for the phenolic hydroxyl group, which seriously disrupts the ESIPT process between the keto and enol tautomers so that only one higher energy emission band assigned to the enol tautomer is found. On the other hand, the rotation of the C–C bond between the two aryl moieties in 2-hydroxy-phenyl-1,3,4-oxadiazole brings intramolecular radiationless transition, which weakens the emission of phenyl-1,3,4-oxadiazole. Therefore, **1** appears to be a promising candidate for enhancing fluorescence emission upon binding



Scheme 1 Synthesis of fluorescent chemosensor **1**.

suitable metal ions, if their radiationless channel could be well blocked.

To gain insight into the chemosensing properties and coordination mechanism of **1** towards metal ions in the solution, the spectrophotometric titration was investigated in aprotic acetonitrile. Fig. 1a shows gradual changes in the absorption spectra of **1** upon addition of  $\text{Zn}^{2+}$ . The absorbance of **1** at 209, 275 and 314 nm decreases markedly and two new absorption peaks at 245 and 364 nm gradually increase with increasing concentration of  $\text{Zn}^{2+}$ , accompanied by the formation of four isosbestic points at 216, 257, 296 and 333 nm. It is expected to correspond to the coordination of **1** with  $\text{Zn}^{2+}$ , which extends the conjugated system and results in the appearance of the new absorption in the long wavelength region. In addition, the absorbance at 364 nm with the increase of  $[\text{Zn}^{2+}]$  shows a linear enhancement when the ratio of  $[\text{Zn}^{2+}]/[\mathbf{1}]$  is below 1 : 1, but no longer change when the ratio reaches higher than 5 : 1. The intersection point of two best-fit straight lines is at the ratio of 1 : 1, assuming 1 : 1 stoichiometry between **1** and  $\text{Zn}^{2+}$  (inset, Fig. 1a). Furthermore, the association constant of **1**– $\text{Zn}^{2+}$  complex system was estimated to

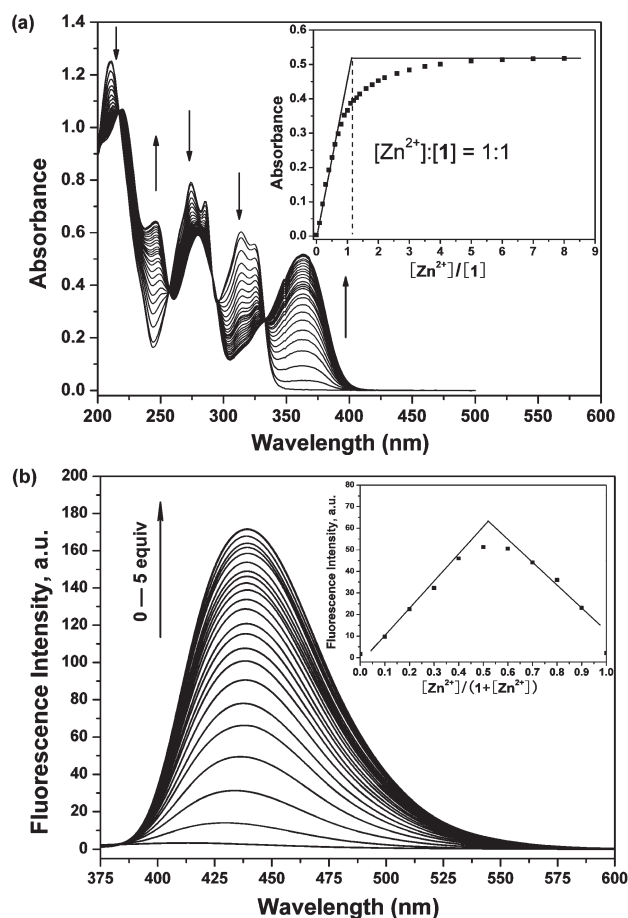


Fig. 1 (a) Absorption spectra of **1** in acetonitrile with the increase of  $\text{Zn}(\text{ClO}_4)_2$ . Inset: The absorbance at 364 nm varied as a function of  $[\text{Zn}^{2+}]/[\mathbf{1}]$ .  $[\mathbf{1}] = 5.0 \times 10^{-5}$  M. (b) Fluorescence spectra of **1** in acetonitrile in the presence of increasing concentration of  $\text{Zn}(\text{ClO}_4)_2$ .  $[\mathbf{1}] = 5.0 \times 10^{-5}$  M. Inset: Job's plot for determining the stoichiometry of **1** and  $\text{Zn}^{2+}$ . The total concentration ( $[\mathbf{1}] + [\text{Zn}^{2+}]$ ) was  $5.0 \times 10^{-5}$  M.  $\lambda_{\text{ex}} = 333$  nm.

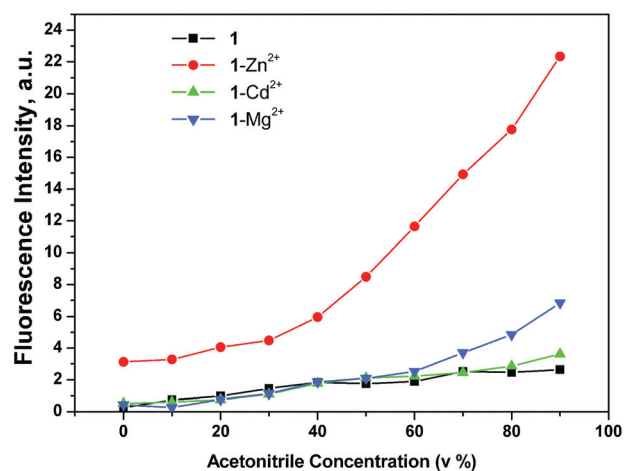
be  $1.7 \times 10^5 \text{ M}^{-1}$  by nonlinear fitting of the data according to the absorbance titration curve at 364 nm ( $R^2 = 0.9953$ , Fig. S1†).

Fig. 1b shows gradual changes in the fluorescence spectra of **1** upon addition of  $\text{Zn}^{2+}$  under excitation at 333 nm, which is one of the isosbestic points in the absorption spectra. The fluorescence intensity increases remarkably and a fluorescence enhancement factor at 439 nm of approximately 65-fold is estimated. These changes in the fluorescence spectra almost stopped and the emission intensities became constant when the amount of  $\text{Zn}^{2+}$  added reached 5 equiv, and an obvious red shift of the  $\lambda_{\text{max,em}}$  from 410 to 439 nm could be observed. The association constant of **1**– $\text{Zn}^{2+}$  complex system was also estimated to be  $1.6 \times 10^5 \text{ M}^{-1}$ , close to the value obtained by the absorbance titration curve at 364 nm (Fig. S2†). Job's plot analysis of the fluorescence for **1**– $\text{Zn}^{2+}$  system exhibits a maximum at about 0.5 mole fraction, in accord with the proposed 1 : 1 stoichiometry (Fig. 1b, inset).

Compared with a fluorescence titration with  $\text{Zn}^{2+}$ , it is noted that in pure acetonitrile under excitation at 333 nm, the  $\lambda_{\text{max,em}}$  of **1** undergoes a 20 nm red-shift and fluorescence enhancement about 2-fold with increasing concentration of  $\text{Cd}^{2+}$  (Fig. S3†), but a slight 10 nm red-shift and evident fluorescence enhancement about 20-fold at 420 nm in the presence of  $\text{Mg}^{2+}$  (Fig. S6†). Other metal ions cannot cause this fluorescent OFF–ON change. The association constant for  $\text{Cd}^{2+}$  and  $\text{Mg}^{2+}$  were estimated to be  $1.7 \times 10^4 \text{ M}^{-1}$  and  $4.8 \times 10^4 \text{ M}^{-1}$  on the basis of nonlinear fitting of the absorbance titration at  $\sim 365$  nm with a 1 : 1 stoichiometry, respectively, which are smaller than that for  $\text{Zn}^{2+}$  (Fig. S5 and S8†). The similarities of the absorbance changes and fluorescence responses for the three metal ions suggest that **1** could coordinate with  $\text{Cd}^{2+}$  and  $\text{Mg}^{2+}$  to form complex like **1**– $\text{Zn}^{2+}$  as a result of the deprotonation of the phenolic hydroxyl of **1** in aprotic solvent to some extent, but the stabilities of different complex systems are obviously distinct.

Generally, one of the most practical applications for a fluorescent probe is the detection of metal ions in aqueous solution, therefore the fluorescence recognition of **1** in a  $\text{CH}_3\text{CN}$ – $\text{H}_2\text{O}$  binary solvent mixture was carried out. More interestingly, the increase of the water content in the mixed solvent led to the fluorescence quenching of **1**– $\text{Zn}^{2+}$  complex to a certain extent, but the fluorescence response signal of **1** for  $\text{Zn}^{2+}$  was still obvious compared with the probes own fluorescence. Moreover, the higher water content could effectively exclude CHEF interference of  $\text{Cd}^{2+}$  and  $\text{Mg}^{2+}$  so that the specificity of fluorescence OFF–ON of **1** for  $\text{Zn}^{2+}$  was significantly improved (Fig. 2, Fig. S9 and S10†). This phenomenon may be attributed to the formation of metal ion hydrate species or the presence of plenty of intermolecular hydrogen bonding in the protic water-based mixed solvent, which easily results in complete dissociation of unstable **1**– $\text{Cd}^{2+}$  or **1**– $\text{Mg}^{2+}$  complexes and partial dissociation of **1**– $\text{Zn}^{2+}$  complex accompanied with the quenching of fluorescence. The explanation could be confirmed clearly by the significant absorbance changes of **1** between 340 nm and 400 nm only while adding  $\text{Zn}^{2+}$  (Fig. S11†).

Fluorescent sensors based on electron donors/acceptors are usually disturbed by protons in the detection of metal ions, so the fluorescence intensity of **1** at various pH values in the presence and absence of  $\text{Zn}^{2+}$  were measured to search for the “turn-off state” and find optimal application conditions in 50%



**Fig. 2** Effect of water content on the fluorescence intensity of **1** (50  $\mu\text{M}$ ) in the presence of  $\text{Zn}^{2+}$ ,  $\text{Cd}^{2+}$  and  $\text{Mg}^{2+}$  ions (5 equiv) in  $\text{CH}_3\text{CN}$ – $\text{H}_2\text{O}$  binary solvent mixture. The  $\lambda_{\text{max,em}}$  are 425 nm for **1**, 437 nm for **1**– $\text{Zn}^{2+}$ , 425 nm for **1**– $\text{Mg}^{2+}$  and 430 nm for **1**– $\text{Cd}^{2+}$ , respectively.  $\lambda_{\text{max,ex}} = 363$  nm.

$\text{CH}_3\text{CN}$ – $\text{H}_2\text{O}$  mixed solvent (Fig. S12†). The results showed that no dramatic fluorescence change for **1** and **1**– $\text{Zn}^{2+}$  system under acidic conditions because of protonation of the phenolic hydroxyl and 1,3,4-oxadiazole nitrogen atom of **1**, leading to a weak coordinating ability of  $\text{Zn}^{2+}$ . However, satisfactory  $\text{Zn}^{2+}$ -sensing abilities were exhibited when the pH was at neutral and under weakly alkaline conditions. Thus, **1** displayed good fluorescence sensing ability to  $\text{Zn}^{2+}$ , which makes it suitable for application in physiological conditions.

Fig. 3a shows the fluorescence spectra of the sensor **1** (10  $\mu\text{M}$ ) when measured in a buffered  $\text{CH}_3\text{CN}$ – $\text{H}_2\text{O}$  mixture (1 : 1 v/v; HEPES 10 mM; pH 7.2) with respective metal cations. Upon the addition of an excess of 10 equiv of various metal ions, including  $\text{Ca}^{2+}$ ,  $\text{Cd}^{2+}$ ,  $\text{Co}^{2+}$ ,  $\text{Cr}^{3+}$ ,  $\text{Cu}^{2+}$ ,  $\text{Fe}^{3+}$ ,  $\text{Hg}^{2+}$ ,  $\text{K}^+$ ,  $\text{Li}^+$ ,  $\text{Mg}^{2+}$ ,  $\text{Mn}^{2+}$ ,  $\text{Na}^+$ ,  $\text{Ni}^{2+}$ ,  $\text{Pb}^{2+}$  and  $\text{Zn}^{2+}$  (as their  $\text{ClO}_4^-$  salts), only a clear fluorescence enhancement (*ca.* 5-fold) was observed for  $\text{Zn}^{2+}$ , but no increase of fluorescent emission in the same conditions for other metal ions. There was partial fluorescence quenching for  $\text{Cu}^{2+}$ ,  $\text{Cr}^{3+}$ ,  $\text{Fe}^{3+}$  and  $\text{Hg}^{2+}$ , which may be due to non-radiative energy transition in the process of electron or energy transfer between the d orbital of the ions and the fluorophore. Furthermore, tolerance of the fluorescence intensity for  $\text{Zn}^{2+}$  (10  $\mu\text{M}$ ) in the presence of an excess of human body required metal ions (1 mM) like  $\text{Na}^+$ ,  $\text{K}^+$ ,  $\text{Ca}^{2+}$  and  $\text{Mg}^{2+}$  has been successfully verified, with no effects on the fluorescence intensity (Fig. 3b).

When **1** was employed at 50  $\mu\text{M}$  and the slit was adjusted to 5.0 nm/5.0 nm, the linear dynamic response concentration range for  $\text{Zn}^{2+}$  covers from  $5.0 \times 10^{-6}$  to  $5.0 \times 10^{-5}$  M in HEPES buffer (10 mM, pH = 7.2,  $\text{CH}_3\text{CN}$ – $\text{H}_2\text{O} = 1 : 1$ , v/v) (Fig. S13†). The detection limit (LOD) and quantification limit (LOQ) were measured to be  $2.2 \times 10^{-7}$  M ( $3\sigma/\text{slope}$ ) and  $7.3 \times 10^{-7}$  M ( $10\sigma/\text{slope}$ ), respectively. The association constant of the **1**– $\text{Zn}^{2+}$  complex system was estimated to be  $5.3 \times 10^3 \text{ M}^{-1}$  by nonlinear fitting of the fluorescence titration curve with 1 : 1 stoichiometry (Fig. 4). In addition, the interaction of **1** with  $\text{Zn}^{2+}$

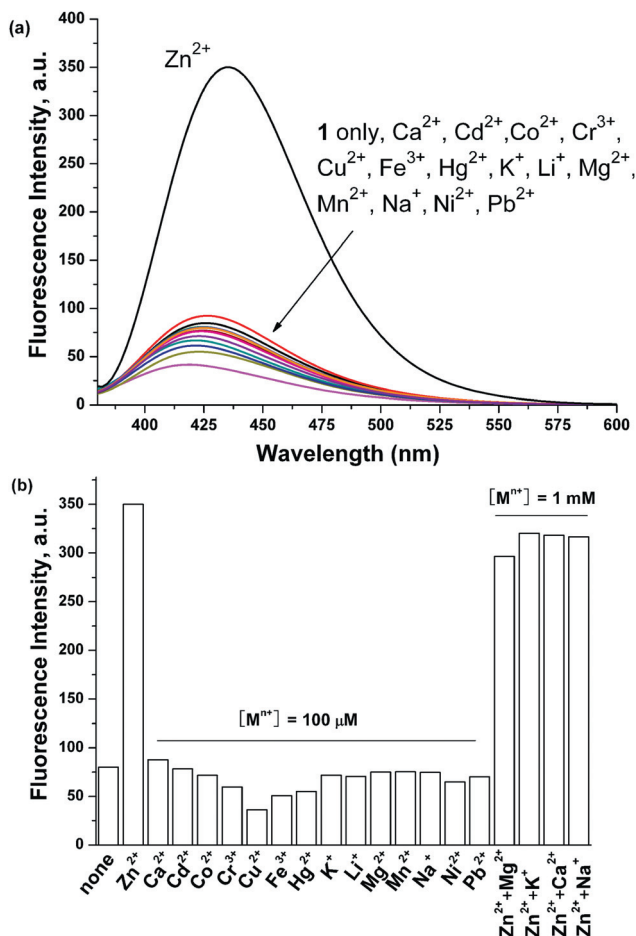


**Fig. 3** (a) Fluorescence spectra of **1** (10  $\mu\text{M}$ ) in the presence of different metal ions (10 equiv, as their  $\text{Cl}^-$  or  $\text{ClO}_4^-$  salts) in HEPES buffer (10 mM, pH = 7.2,  $\text{CH}_3\text{CN}-\text{H}_2\text{O} = 1:1$ , v/v). (b) Relative fluorescence intensity change profile of **1** (10  $\mu\text{M}$ ) in the presence of various metal ions in HEPES buffer (10 mM, pH = 7.2,  $\text{CH}_3\text{CN}-\text{H}_2\text{O} = 1:1$ , v/v). The final concentration for  $\text{Zn}^{2+}$ ,  $\text{Cd}^{2+}$ ,  $\text{Co}^{2+}$ ,  $\text{Cr}^{3+}$ ,  $\text{Cu}^{2+}$ ,  $\text{Fe}^{3+}$ ,  $\text{Hg}^{2+}$ ,  $\text{Li}^+$ ,  $\text{Mn}^{2+}$ ,  $\text{Ni}^{2+}$  and  $\text{Pb}^{2+}$  is 100  $\mu\text{M}$ , for  $\text{Na}^+$ ,  $\text{K}^+$ ,  $\text{Ca}^{2+}$  and  $\text{Mg}^{2+}$  is 1 mM.  $\lambda_{\text{max}}\text{ex} = 363$  nm.

was completed in a few seconds, therefore **1** has the favorable property required for intracellular  $\text{Zn}^{2+}$  imaging.

To understand the selectivity fluorescence enhancement of **1** for  $\text{Zn}^{2+}$  and the configuration of **1**- $\text{Zn}^{2+}$  system, we carried out studies on the time-resolved fluorescence decay of **1** and density functional theory (DFT) calculations of **1**- $\text{Zn}^{2+}$ .

The decay curve of the fluorescence intensity of **1** and fitting data were shown in Fig. 5. The result suggested that there were three main isomer components (*enol* torsion tautomer, *enol* rotamer, *enol* tautomer) of **1** to absorb the excitation light and emit fluorescence photons of different lifetime about 0.33 ns, 2.24 ns and 6.77 ns, respectively. The average fluorescence lifetime ( $\tau$ ) of **1** was estimated as 3.20 ns (Table S1†). In the presence of  $\text{Zn}^{2+}$  (**1**: $\text{Zn}^{2+} = 1:5$ ), the time-resolved fluorescence decay showed significant change according to the steady state fluorescence spectra, which indicated that plenty of a new component corresponding to  $\text{Zn}^{2+}$ -complex at 4.19 ns was formed and a small number of *enol* rotamer components of **1** at 2.52 ns ( $\sim 2.24$  ns) still remained. A longer average fluorescence lifetime

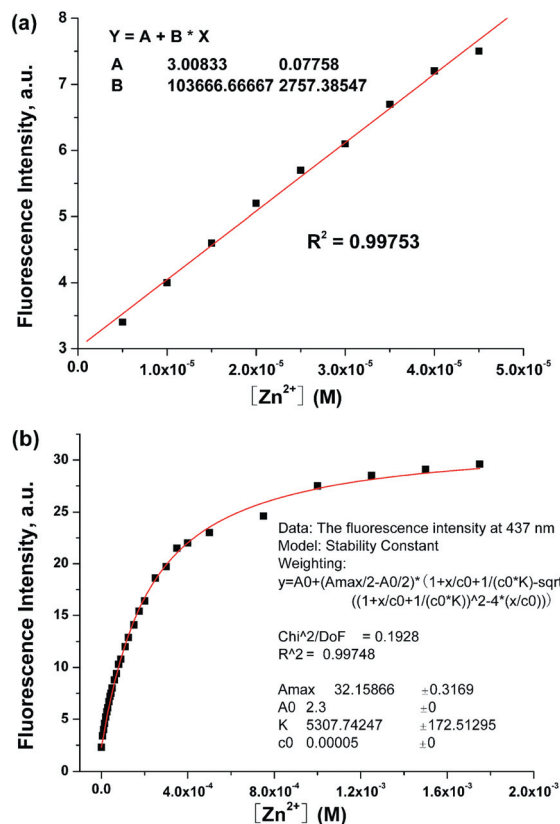


**Fig. 4** (a) The linear dynamic response of **1** for  $\text{Zn}^{2+}$  and the determination of the detection limit (LOD) for  $\text{Zn}^{2+}$  in HEPES buffer (10 mM, pH = 7.2,  $\text{CH}_3\text{CN}-\text{H}_2\text{O} = 1:1$ , v/v). The LOD was calculated by multiplying the standard deviation of 11 blank measurements by three and dividing by the slope of the linear calibration curve in lower concentration. (b) Change in the fluorescence intensity at 437 nm. The red line is the nonlinear fitting curve obtained assuming a 1:1 association between **1** and  $\text{Zn}^{2+}$ .  $\lambda_{\text{max}}\text{ex} = 363$  nm,  $[\mathbf{1}] = 5.0 \times 10^{-5}$  M.

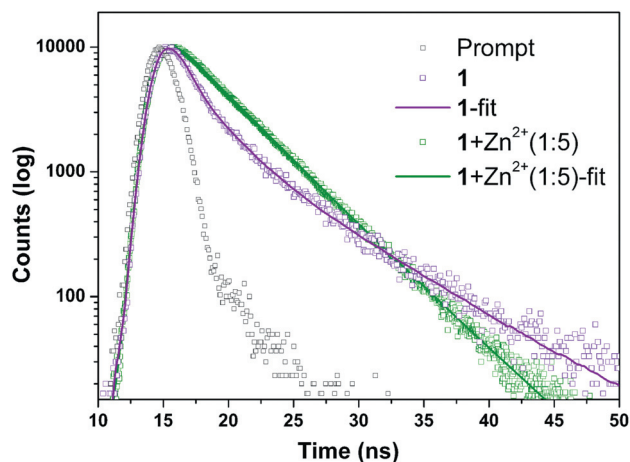


**Fig. 5** Time-resolved fluorescence decay of **1** in the absence and presence of added  $\text{Zn}^{2+}$ .  $\lambda_{\text{ex}} = 350$  nm.

(3.99 ns) was detected. According to the equations  $\tau^{-1} = k_r + k_{nr}$  and  $k_r = \Phi_f/\tau$ , the radiative rate constant  $k_r$  and the total non-radiative rate constant  $k_{nr}$  of **1** and  $\text{Zn}^{2+}$ -bound species were

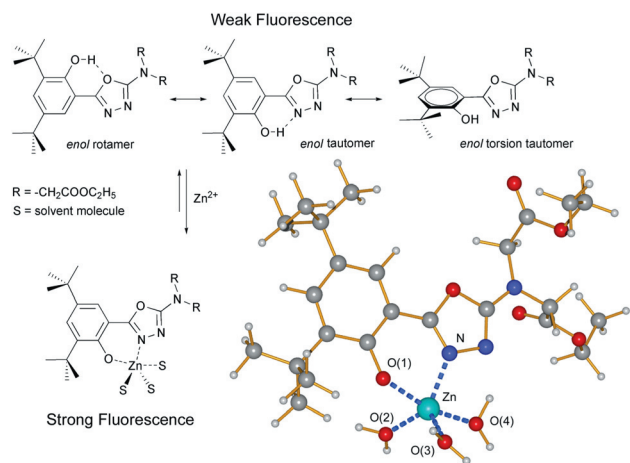


**Fig. 6** Chemical structures related with *enol* torsion tautomer, *enol* rotamer, *enol* tautomer, complex, and calculated energy-minimized structure of **1** with  $\text{Zn}^{2+}$ .

calculated and listed in Table S1.<sup>†19</sup> The data suggest that the factor that induces fluorescent enhancement is mainly ascribed to the formation of a new complex with rigid planar structure and more than 3.5 times increase of  $k_r$ , whereas the tautomerism and rotational isomerization of **1** are wholly or partially blocked.

DFT calculations with B3LYP exchange functionals were performed by using the Gaussian 09 package. The 6-31G basis sets were used except for  $\text{Zn}^{2+}$ , where LANL2DZ effective core potential (ECP) was employed. The optimized configuration is shown in Fig. 6, which shows that the  $\text{Zn}^{2+}$  ion is well chelated by the O atom of the phenolic hydroxyl group and N atom of the 1,3,4-oxadiazole of **1**, and torsional motions of the two aryl moieties could be effectively prevented, accompanied by the formation of rigid planar structure. The Zn–N bond length is 2.07 Å and Zn–O bond lengths are 2.07 Å (Zn–O phenolic), 2.07 Å, 2.01 Å and 2.13 Å (Zn–O solvents  $\text{H}_2\text{O}$ ), respectively. These data indicate that  $\text{Zn}^{2+}$  ions can effectively electrophilic attack the hydroxyl oxygen atom with electron-rich property of **1** to simultaneously block the nonradiative transitions to turn on the fluorescence signal.

The intracellular  $\text{Zn}^{2+}$  imaging behavior of **1** was studied on the Hep G2 (liver cancer) cells by fluorescence microscopy. As shown in Fig. 7, after incubation with compound **1** (10  $\mu\text{M}$  in DMEM) at 25 °C for 30 min, the cells displayed very faint intracellular fluorescence. However, cells exhibited intensive fluorescence when exogenous  $\text{Zn}^{2+}$  was introduced into the cell *via* incubation with a  $\text{Zn}(\text{NO}_3)_2$  (10  $\mu\text{M}$  in DMEM) under the same conditions after 30 min. It is suggested that chemosensor **1** could easily permeate the cell membrane and coordinate with  $\text{Zn}^{2+}$  ion in living cell organizations so that the fluorescence showed evident change. Hence, these results indicate that **1** is an efficient candidate to monitor the important role of  $\text{Zn}^{2+}$  under biological conditions and in aqueous solution.

## Conclusions

In conclusion, an aromatic 1,3,4-oxadiazole-based fluorescence chemosensor **1** was designed and synthesized. The chemosensor

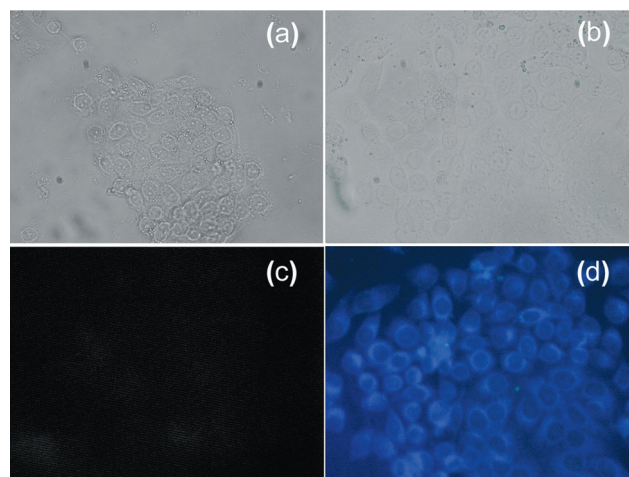


**Fig. 7** Bright field images of the Hep G2 cells loaded with **1** (10  $\mu\text{M}$  in DMEM) incubated for 30 min (a) without and (b) with the addition of  $\text{Zn}^{2+}$  (1 equiv); Fluorescence microscope images of the Hep G2 cells loaded with **1** incubated for 30 min (c) without and (d) with the addition of  $\text{Zn}^{2+}$  (1 equiv).

**1** could coordinate with  $\text{Zn}^{2+}$  *via* a 1 : 1 binding mode and only display high selective and sensitive fluorescence response to  $\text{Zn}^{2+}$  over other metal ions in aqueous acetonitrile solution or HEPES buffer. It was found that the process of OFF–ON fluorescence enhancement mostly is ascribed to stable electrophilic attack of  $\text{Zn}^{2+}$  ion to the phenolic oxygen atom with electron-rich property and effective prevention of torsional motions of the two aryl moieties in the 2-hydroxy-phenyl-1,3,4-oxadiazole group, accompanying the formation of new complex with rigid planar structure and blocking of non-radiative transitions. The fluorescence imaging of  $\text{Zn}^{2+}$  in living cells was successfully applied by using fluorescence confocal microscopy, and the results revealed that the chemosensor can be utilized in living cells for monitoring  $\text{Zn}^{2+}$ .

## Experimental section

### Materials and general methods

All the materials for synthesis were purchased from commercial suppliers and used without further purification. All of the solvents used were of analytical reagent grade and deionized water was used. All metal salts used were perchlorates of general formula  $\text{M}(\text{ClO}_4)_n \cdot x\text{H}_2\text{O}$  formula, and NaCl, KCl,  $\text{MgCl}_2 \cdot 6\text{H}_2\text{O}$  and  $\text{CaCl}_2$  were also used in the competition experiments in HEPES buffer. HEPES buffer solutions (10 mM, pH = 7.2) were prepared in  $\text{CH}_3\text{CN}-\text{H}_2\text{O}$  (1 : 1, v/v).  $^1\text{H}$  and  $^{13}\text{C}$  NMR spectra were taken on a Varian mercury-300 spectrometer with TMS as an internal standard and  $\text{CDCl}_3$  as solvent. Mass spectra were recorded on a Bruker Daltonics esquire6000 Mass spectrometer. Quantum yields were determined by an absolute method using an integrating sphere on an Edinburgh Instrument FLS920. The fluorescence lifetimes were determined with an Edinburgh Instrument FLS920 fluorescence spectrophotometer using a nanosecond-pulsed flashlamp as the light source. Fluorescence spectra measurements were performed on a Hitachi F-4500

spectrofluorimeter equipped with quartz cuvettes of 1 cm path length with a xenon lamp as the excitation source. Absorption spectra were recorded on a Varian UV-Cary100 spectrophotometer using quartz cells of 1.0 cm path length. IR spectra were recorded on Nicolet FT-170SX instrument using KBr discs in the 400–4000  $\text{cm}^{-1}$  region. All pH measurements were made with a pH-10C digital pH meter. All spectra were recorded at 20 °C. Fluorescence microscopy experiments were performed on a fluorescence microscope (DMI 4000 B, Leica Microsystem) with excitation between 340–380 nm. The total magnification was 400 $\times$ .

### Preparation of ligand

**1-(3,5-Di-*tert*-butyl-2-hydroxybenzylidene)semicarbazide (3).** To a stirred solution of semicarbazide hydrochloride (3.06 g, 27.5 mmol) and NaOH (1.1 g, 27.5 mmol) in 10 mL water was added dropwise a solution of 3,5-di-*tert*-butyl-2-hydroxybenzaldehyde (5.85 g, 25.0 mmol) in 40 mL ethanol at 65 °C. The reaction mixture was refluxed for 8 h and then cooled to room temperature. Yellow precipitates formed were filtered and washed with water and ethanol, then dried under vacuum. Yield: 89.3% (6.5 g). Mp: 180.0–182.5 °C. FT-IR (KBr phase) ( $\text{cm}^{-1}$ ): 3425 s, 2960 s, 1676 vs, 1587 s, 1437 vs, 1363 m, 1246 m, 1206 w, 1174 w, 1103 w, 1031 w, 954 w, 828 w, 764 w, 644 w.

**5-(2-Hydroxy-3,5-di-*tert*-butylphenyl)-[1,3,4]oxadiazol-2-amine (2).** To a stirred suspension of **3** (5.82 g, 20.0 mmol) and anhydrous sodium acetate (6.58 g, 20.0 mmol) in 24 mL glacial acetic acid was added dropwise slowly a solution of  $\text{Br}_2$  (1.14 mL, 22.0 mmol) in 4 mL glacial acetic acid at room temperature. After further stirring for 4 h, the reaction mixture was poured into 300 mL of ice water. The precipitates were filtered and washed with lots of water. The pale yellow product was dried under vacuum. Yield: 93.4% (5.4 g). Mp: 236.5–238.5 °C. FT-IR (KBr phase) ( $\text{cm}^{-1}$ ): 3434 vs, 2961 m, 1656 vs, 1617 m, 1554 m, 1462 w, 1433 m, 1293 w, 1362 w, 1253 m, 1221 w, 1098 w, 986 w, 882 w, 770 w, 645 w.  $^1\text{H}$  NMR (200 MHz,  $\text{CDCl}_3$ , ppm):  $\delta$  1.46 (9H, s,  $-\text{C}(\text{CH}_3)_3$ ), 1.58 (9H, s,  $-\text{C}(\text{CH}_3)_3$ ), 5.15 (2H, s,  $-\text{NH}_2$ ), 7.44–7.45 (2H, Ar–H), 10.27 (1H, s,  $-\text{OH}$ ).  $^{13}\text{C}$  NMR (50 MHz,  $\text{CDCl}_3$ , ppm):  $\delta$  28.79, 30.83, 33.71, 34.62, 107.28, 119.26, 126.65, 136.51, 140.78, 153.20, 159.63, 161.15. ESI-MS:  $m/z$  290.3 ( $\text{M} + \text{H}^+$ ).

***N*-(2-Ethoxy-2-oxoethyl)-*N*-(5-(2-hydroxy-3,5-di-*tert*-butylphenyl)-[1,3,4]oxadiazol-2-yl)glycine ethyl ester (1).** Anhydrous potassium carbonate (0.69 g, 5 mmol) was added to a solution of **2** (0.289 g, 1 mmol) in acetonitrile (25 mL), and the mixture was held at reflux. An hour later, a 5 mL acetonitrile solution containing ethyl chloroacetate (0.61 g, 5 mmol) was added to the mixture (excess of ethyl chloroacetate for improving the yield of the ligand **1**). The reaction mixture was held at reflux for another 5 h and then cooled to room temperature. The insoluble inorganic carbonate was removed by vacuum filtering and washed by acetonitrile. The filtrate was evaporated under reduced pressure, and the mixture was purified by silica gel column chromatography using 5 : 1 (v/v) petroleum ether–ethyl acetate to afford **1** as pale yellow viscous liquid. Yield: 75.0% (0.35 g).  $^1\text{H}$  NMR (200 MHz,  $\text{CDCl}_3$ , ppm):  $\delta$  1.27–1.34 (15H, m,

$-\text{C}(\text{CH}_3)_3$  and  $-\text{CH}_3$ ), 1.45 (9H, s,  $-\text{C}(\text{CH}_3)_3$ ), 4.20–4.31 (4H, q,  $-\text{CH}_2-$ ), 4.37 (4H, s,  $-\text{CH}_2-$ ), 7.37 (1H, s, Ar–H), 7.41 (1H, s, Ar–H), 10.24 (1H, s,  $-\text{OH}$ ).  $^{13}\text{C}$  NMR (50 MHz,  $\text{CDCl}_3$ , ppm):  $\delta$  14.14, 29.38, 31.41, 34.25, 35.23, 50.75, 61.74, 107.89, 119.57, 127.22, 137.13, 141.24, 153.80, 160.61, 162.31, 168.43. ESI-MS:  $m/z$  462.5 ( $\text{M} + \text{H}^+$ ).

### Acknowledgements

The authors acknowledge the financial support from the NSFC (Grants 20931003, 91122007, 21001059), the Specialized Research Fund for the Doctoral Program of Higher Education (Grant No. 20110211130002) and the Fundamental Research Funds for the Central Universities (Izujbky-2012-70, Izujbky-2012-189).

### Notes and references

- (a) *Fluorescent Chemosensors for Ion and Molecule Recognition*, ed. A. W. Czarnik, American Chemical Society, Washington, DC, 1992; (b) J. P. Desvergne and A. W. Czarnik, *Chemosensors of Ion and Molecule Recognition*, Kluwer, Dordrecht, 1997; (c) A. P. de Silva, H. Q. N. Gunaratne, T. Gunnlaugsson, A. J. M. Huxley, C. P. McCoy, J. T. Rademacher and T. E. Rice, *Chem. Rev.*, 1997, **97**, 1515–1566; (d) V. Amendola, L. Fabbrizzi, F. Forti, M. Licchelli, C. Mangano, P. Pallavicini, A. Poggi, D. Sacchi and A. Taglieti, *Coord. Chem. Rev.*, 2006, **250**, 273–299; (e) C. Lodeiro, J. L. Capelo, J. C. Mejuto, E. Oliveira, H. M. Santos, B. Pedras and C. Nunez, *Chem. Soc. Rev.*, 2010, **39**, 2948–2976.
- (a) S. J. Lippard and J. M. Berg, *Principles of Bioinorganic Chemistry*, University Science Books, Mill Valley, CA, 1994; (b) J. M. Berg and Y. Shi, *Science*, 1996, **271**, 1081–1085; (c) A. P. de Silva, D. B. Fox, A. J. M. Huxley and T. S. Moody, *Coord. Chem. Rev.*, 2000, **205**, 41–57; (d) D. S. Auld, *BioMetals*, 2001, **14**, 271–313; (e) Z. K. Wu, Y. F. Zhang, J. S. Ma and G. Q. Yang, *Inorg. Chem.*, 2006, **45**, 3140–3142.
- (a) S. Y. Assaf and S. H. Chung, *Nature*, 1984, **308**, 734–736; (b) G. A. Howell, M. G. Welch and C. J. Frederickson, *Nature*, 1984, **308**, 736–738; (c) T. V. O'Halloran, *Science*, 1993, **261**, 715–725; (d) J. Y. Koh, S. W. Suh, B. J. Gwag, Y. Y. He, C. Y. Hsu and D. W. Choi, *Science*, 1996, **272**, 1013–1016; (e) S. W. Suh, K. B. Jensen, M. S. Jensen, D. S. Silva, P. J. Kesslak, G. Danscher and C. J. Frederickson, *Brain Res.*, 2000, **852**, 274–278; (f) C. J. Frederickson and A. I. Bush, *BioMetals*, 2001, **14**, 353–366; (g) W. J. Qian, K. R. Gee and R. T. Kennedy, *Anal. Chem.*, 2003, **75**, 3468–3475; (h) C. F. Walker and R. E. Black, *Annu. Rev. Nutr.*, 2004, **24**, 255–275; (i) C. J. Frederickson, J.-Y. Koh and A. I. Bush, *Nat. Rev. Neurosci.*, 2005, **6**, 449–462.
- (a) N. C. Lim, H. C. Freake and C. Brückner, *Chem.–Eur. J.*, 2005, **11**, 38–49; (b) Z. Dai and J. W. Canary, *New J. Chem.*, 2007, **31**, 1708–1718; (c) E. L. Que, D. W. Domaille and C. J. Chang, *Chem. Rev.*, 2008, **108**, 1517–1549; (d) Z. Xu, J. Yoon and D. R. Spring, *Chem. Soc. Rev.*, 2010, **39**, 1996–2006; (e) E. Tomat and S. J. Lippard, *Curr. Opin. Chem. Biol.*, 2010, **14**, 225–230; (f) H. G. Lee, J. H. Lee, S. P. Jang, H. M. Park, S. Kim, Y. Kim, C. Kim and R. G. Harrison, *Tetrahedron*, 2011, **67**, 8073–8078.
- (a) B. Tang, H. Huang, K. Xu, L. Tong, G. Yang, X. Liu and L. An, *Chem. Commun.*, 2006, 3609–3611; (b) S. Atilgan, T. Ozdemir and E. U. Akkaya, *Org. Lett.*, 2008, **10**, 4065–4067; (c) Z.-X. Han, X.-B. Zhang, Z. Li, Y.-J. Gong, X.-Y. Wu, Z. Jin, C.-M. He, L.-X. Jian, J. Zhang, G.-L. Shen and R.-Q. Yu, *Anal. Chem.*, 2010, **82**, 3108–3113; (d) Y. Xu and Y. Pang, *Chem. Commun.*, 2010, **46**, 4070–4072; (e) J. Zhu, H. Yuan, W. Chan and A. W. M. Lee, *Org. Biomol. Chem.*, 2010, **8**, 3957–3964; (f) U. C. Saha, B. Chattopadhyay, K. Dhara, S. K. Mandal, S. Sarkar, A. R. Khuda-Bukhsh, M. Mukherjee, M. Helliwell and P. Chattopadhyay, *Inorg. Chem.*, 2011, **50**, 1213–1219.
- (a) C. J. Frederickson, E. J. Kasarskis, D. Ringo and R. E. Frederickson, *J. Neurosci. Methods*, 1987, **20**, 91–103; (b) M. C. Kimber, I. B. Mahadevan, S. F. Lincoln, A. D. Ward and W. H. Betts, *Aust. J. Chem.*, 2001, **54**, 43–49; (c) Y. Zhang, X. Guo, W. Si, L. Jia and

- X. Qian, *Org. Lett.*, 2008, **10**, 473–476; (d) I. Ravikumar and P. Ghosh, *Inorg. Chem.*, 2011, **50**, 4229–4231; (e) E. Hao, T. Meng, M. Zhang, W. Pang, Y. Zhou and L. Jiao, *J. Phys. Chem. A*, 2011, **115**, 8234–8241; (f) J. Zhu, W. Chan and A. W. M. Lee, *Tetrahedron Lett.*, 2012, **53**, 2001–2004; (g) G. Xie, Y. Shi, F. Hou, H. Liu, L. Huang, P. Xi, F. Chen and Z. Zeng, *Eur. J. Inorg. Chem.*, 2012, 327–332.
- 7 (a) G. K. Walkup, S. C. Burdette, S. J. Lippard and R. Y. Tsien, *J. Am. Chem. Soc.*, 2000, **122**, 5644–5645; (b) S. C. Burdette, G. K. Walkup, B. Spingler, R. Y. Tsien and S. J. Lippard, *J. Am. Chem. Soc.*, 2001, **123**, 7831–7841; (c) C. J. Chang, E. M. Nolan, J. Jaworski, S. C. Burdette, M. Sheng and S. J. Lippard, *Chem. Biol.*, 2004, **11**, 203–210; (d) X. Meng, M. Zhu, L. Liu and Q. Guo, *Tetrahedron Lett.*, 2006, **47**, 1559–1562.
- 8 (a) N. C. Lim and C. Brückner, *Chem. Commun.*, 2004, 1094–1095; (b) J. P. Goddard and J. L. Raymond, *Trends Biotechnol.*, 2004, **22**, 363–370; (c) H. E. Katerinopoulos, *Curr. Pharm. Des.*, 2004, **10**, 3835–3852; (d) N. C. Lim, J. V. Schuster, M. C. Porto, M. A. Tanudra, L. Yao, H. C. Freake and C. Brückner, *Inorg. Chem.*, 2005, **44**, 2018–2030; (e) L. Zhang, S. Dong and L. Zhu, *Chem. Commun.*, 2007, 1891–1893; (f) K. Komatsu, Y. Urano, H. Kojima and T. Nagano, *J. Am. Chem. Soc.*, 2007, **129**, 13447–13454; (g) S. Mizukami, S. Okada, S. Kimura and K. Kikuchi, *Inorg. Chem.*, 2009, **48**, 7630–7638.
- 9 (a) A. Bencini, E. Berni, A. Bianchi, P. Fornasari, C. Giorgi, J. C. Lima, C. Lodeiro, M. J. Melo, J. S. de Melo, A. J. Parola, F. Pina, J. Pina and B. Valtancoli, *Dalton Trans.*, 2004, 2180–2187; (b) Y. Shiraiishi, Y. Kohno and T. Hirai, *J. Phys. Chem. B*, 2005, **109**, 19139–19147; (c) F. Zapata, A. Caballero, A. Espinosa, A. Tárraga and P. Molina, *Org. Lett.*, 2007, **9**, 2385–2388.
- 10 (a) J. Wang, Y. Xiao, Z. Zhang, X. Qian, Y. Yang and Q. Xu, *J. Mater. Chem.*, 2005, **15**, 2836–2839; (b) Z. Xu, X. Qian, J. Cui and R. Zhang, *Tetrahedron*, 2006, **62**, 10117–10122; (c) F. Qian, C. Zhang, Y. Zhang, W. He, X. Gao, P. Hu and Z. Guo, *J. Am. Chem. Soc.*, 2009, **131**, 1460–1468; (d) Z. Xu, K. Baek, H. Kim, J. Cui, X. Qian, D. R. Spring, I. Shin and J. Yoon, *J. Am. Chem. Soc.*, 2010, **132**, 601–610; (e) J. F. Zhang, S. Bhuniya, Y. H. Lee, C. Bae, J. H. Lee and J. S. Kim, *Tetrahedron Lett.*, 2010, **51**, 3719–3723.
- 11 (a) M. A. Bernardo, F. Pina, B. Escuder, E. García-España, M. L. Godino-Salido, J. Latorre, S. V. Luis, J. A. Ramirez and C. Soriano, *J. Chem. Soc., Dalton Trans.*, 1999, 915–921; (b) A. Tamayo, C. Lodeiro, L. Escriche, J. Casabó, B. Covelo and P. González, *Inorg. Chem.*, 2005, **44**, 8105–8115; (c) M. Li, H. Lu, R. Liu, J. Chen and C. Chen, *J. Org. Chem.*, 2012, **77**, 3670–3673.
- 12 (a) D. Y. Wu, L. X. Xie, C. L. Zhang, C. Y. Duan, Y. G. Zhao and Z. J. Guo, *Dalton Trans.*, 2006, 3528–3533; (b) M. Hosseini, Z. Vaezi, M. R. Ganjali, F. Faridbod, S. D. Abkenar, K. Alizadeh and M. Salavati-Niasari, *Spectrochim. Acta, Part A*, 2010, **75**, 978–982; (c) N. Li, W. Tang, Y. Xiang, A. Tong, P. Jin and Y. Ju, *Luminescence*, 2010, **25**, 445–451; (d) X. Zhou, B. Yu, Y. Guo, X. Tang, H. Zhang and W. Liu, *Inorg. Chem.*, 2010, **49**, 4002–4007; (e) S. Sakthivel, S. Jammie and T. Punniyamurthy, *Tetrahedron: Asymmetry*, 2012, **23**, 101–107; (f) Y. Zhou, Z. Li, S. Zang, Y. Zhu, H. Zhang, H. Hou and T. C. W. Mak, *Org. Lett.*, 2012, **14**, 1214–1217.
- 13 (a) K. L. Hycr, J. M. Bownik and M. P. Goldberg, *Cell Calcium*, 2000, **27**, 75–86; (b) P. Jiang and Z. Guo, *Coord. Chem. Rev.*, 2004, **248**, 205–229; (c) R. T. Bronson, D. J. Michaelis, R. D. Lamb, G. A. Hussein, P. B. Farnsworth, M. R. Linford, R. M. Izatt, J. S. Bradshaw and P. B. Savage, *Org. Lett.*, 2005, **7**, 1105–1108; (d) X. Tang, X. Peng, W. Dou, J. Mao, J. Zheng, W. Qin, W. Liu, J. Chang and X. Yao, *Org. Lett.*, 2008, **10**, 3653–3656; (e) S. Y. Park, J. H. Yoon, C. S. Hong, R. Souane, J. S. Kim, S. E. Matthews and J. Vicens, *J. Org. Chem.*, 2008, **73**, 8212–8218; (f) K. M. K. Swamy, M. J. Kim, H. R. Jeon, J. Y. Jung and J. Yoon, *Bull. Korean Chem. Soc.*, 2010, **31**, 3611–3616.
- 14 (a) A. W. Czarnik, *Acc. Chem. Res.*, 1994, **27**, 302–308; (b) R. Martínez-Mañez and F. Sancanón, *Chem. Rev.*, 2003, **103**, 4419–4476; (c) J. F. Callan, A. P. de Silva and D. C. Magri, *Tetrahedron*, 2005, **61**, 8551–8588; (d) J. S. Kim and D. T. Quang, *Chem. Rev.*, 2007, **107**, 3780–3799; (e) M. Chen, X. Lv, Y. Liu, Y. Zhao, J. Liu, P. Wang and W. Guo, *Org. Biomol. Chem.*, 2011, **9**, 2345–2349.
- 15 (a) F. A. Omar, N. M. Mahfouz and M. A. Rahman, *Eur. J. Med. Chem.*, 1996, **31**, 819–825; (b) A. Husain, M. S. Y. Khan, S. M. Hasan and M. M. Alam, *Eur. J. Med. Chem.*, 2005, **40**, 1394–1404; (c) B. Narayana, K. K. Vijayaraj, B. V. Ashlatha and N. S. Kumari, *Arch. Pharm.*, 2005, **338**, 373–377; (d) M. Amir and S. Kumar, *Acta Pharm.*, 2007, **57**, 31–45.
- 16 (a) N. K. Chudgar, S. N. Shah and R. A. Vora, *Mol. Cryst. Liq. Cryst.*, 1989, **172**, 51–56; (b) N. N. Math, A. D. Mulla and M. I. Savadatti, *Pramana*, 1991, **36**, 429–434; (c) G. Pistolis and I. Balomenou, *J. Phys. Chem. B*, 2006, **110**, 16428–16438; (d) P. Shih, C. Shu, Y. Tung and Yun Chi, *Appl. Phys. Lett.*, 2006, **88**, 251110.
- 17 (a) Y. Dong, H. Xu, J. Ma and R. Huang, *Inorg. Chem.*, 2005, **44**, 6591–6608; (b) Y. Dong, H. Wang, J. Ma, D. Shen and R. Huang, *Inorg. Chem.*, 2005, **44**, 4679–4692; (c) Y. Ren, C. Du, S. Feng, C. Wang, Z. Kong, B. Yue and H. He, *CrystEngComm*, 2011, **13**, 7143–7148; (d) M. Du, Z. Zhang, C. Li, J. Ribas-Arriño, N. Aliaga-Alcalde and J. Ribas, *Inorg. Chem.*, 2011, **50**, 6850–6852.
- 18 (a) K. Tanaka, T. Kumagai, H. Aoki, M. Deguchi and S. Iwata, *J. Org. Chem.*, 2001, **66**, 7328–7333; (b) M. M. Henary and C. J. Fahrni, *J. Phys. Chem. A*, 2002, **106**, 5210–5220; (c) Y. Tian, C. Chen, C. Yang, A. C. Young, S. Jang, W. Chen and A. K.-Y. Jen, *Chem. Mater.*, 2008, **20**, 1977–1987.
- 19 N. J. Turro, *Modern Molecular Photochemistry*, Benjamin Cummings, Menlo Park, CA, 1978.